

Kinetostatic calibration of a SCARA robot

Serena Ruggeri¹, Angelo Vertuan¹, Giovanni Legnani¹, Antonio Visioli²

¹*Dipartimento di Ingegneria Meccanica e Industriale, Università di Brescia, Italy*

E-mail: serena.ruggeri@ing.unibs.it, angelo.vertuan@ing.unibs.it, giovanni.legnani@ing.unibs.it

²*Dipartimento di Elettronica per l'Automazione, Università di Brescia, Italy*

E-mail: antonio.visioli@ing.unibs.it

Keywords: Industrial robots, calibration, hybrid control.

SUMMARY. In this paper we propose a new algorithm for the kinetostatic calibration of a robot based on contact force measurement. The proposed calibration methodology, called *kinetostatic calibration*, does not require the use of a sensor to measure the robot pose, avoiding all problems related to the use of external devices for this measurement. On the contrary, the robot gripper must be equipped with a force sensor. The robot gripper is requested to touch, with a predefined force, several points of a body of known shape, called *calibration object*. At each contact point, the contact force and the joint rotations are recorded, whereas the end-effector pose can be estimated using a kinetostatic manipulator model. The calibration can be performed on the base of the difference between the measured contact force and that predicted by a model of the manipulator and of the calibration object. In this case the set of the parameters \bar{L} describing the robot includes the geometrical dimensions, the robot compliance and the backlash. After a theoretical introduction, this paper describes the implemented algorithm, the simulations and some experimental results obtained with a SCARA robot.

1 INTRODUCTION

An innovative field of use of industrial manipulators is constituted by applications requiring the interaction between the robot and the environment, such as grinding, assembly or deburring. Performing these tasks, traditional position/velocity control methods may fail. In fact, the force exchanged between robot and environment is very sensitive to the construction tolerances of the manipulator as well as to its compliance. Thus, considering the exchanged force between end-effector and environment is necessary to achieve high performances.

For this purpose, hybrid force-velocity control algorithms can be implemented [1], since one can identify a direction set where the velocity is the controlled variable and a set of orthogonal directions wherein the force is controlled. These control strategies can include the kinematic and dynamic manipulator model, allowing the robot to improve considerably its performances both in terms of execution velocity and accuracy. However, the flaw of these algorithms is that they are based on the accurate knowledge of the elastodynamic manipulator model, achievable through calibration techniques which allow to estimate all the parameters of the model. The standard procedure for the calibration of a general robot is the kinematic calibration [2], [3], based on a

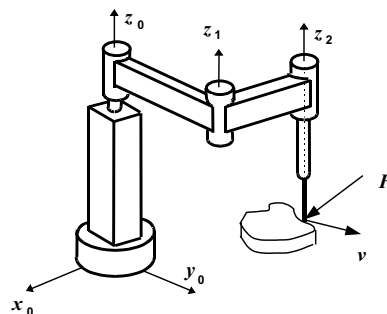


Figure 1: A SCARA robot performing a planar contour tracking.

kinematic model of the robot. In this case the robot compliance and the backlashes are not considered. So, in order to avoid their influence during the process, all measures have to be performed without touching the environment. On the contrary, in this study we are interested in estimating also the robot compliance and the backlashes, and thus it is necessary to exert forces on the gripper. For this reason, we decided to realize a *calibration with contact* [4], [5], based on the measurement of the contact force between robot and environment.

Aim of this paper is then to study a new algorithm for the calibration with contact of industrial manipulators, based on the measurement of both joint coordinates Q and contact forces F . For this purpose, a parametric algorithm has been developed, modelling the system as a chain of rigid bodies with unknown dimensions and connected by joints with concentrated compliance and backlash. Moreover, the gripper compliance and its backlash have been considered in the adopted model. After a theoretical introduction, the procedure is applied to a SCARA robot (figure 1).

2 THE REFERENCE MODEL

2.1 The rigid model

The study of the kinematics and the dynamics of a robot is mostly handled by using rigid body models whose parameters assume predefined constant values (nominal or theoretical values). The kinematic behavior is described by the direct kinematics H and its inverse G , correlating the joints coordinates $Q = [q_1, q_2, \dots]^T$ with the end-effector position $S = [x, y, \dots]^T$:

$$S = H(L, Q) \quad Q = G(L, S) \quad (1)$$

where L is an array of geometrical dimensions describing the manipulator, for example the set of the Denavit and Hartenberg parameters or another set of suitable values. An analysis of the manipulator requires also the use of the jacobian matrix J which correlates the gripper velocity \dot{S} with the joint velocity \dot{Q} , the infinitesimal displacements dS and dQ , and the gripper forces $F = [f_x, f_y, \dots]^T$ with the actuator torques $C = [c_1, c_2, \dots]^T$:

$$J = \frac{\partial S}{\partial Q} \quad \dot{S} = J\dot{Q} \quad dS = JdQ \quad C = J^T F \quad (2)$$

2.2 A deformable model

When the compliance and the backlash of the manipulator cannot be neglected, the gripper position and the joints motions are influenced by the applied forces. After extending the set of the structural parameters to include also a description of the compliance and the backlash, equations (1) and (2) can be extended as:

$$S = H_1(\bar{L}, Q, F) \quad F = H_2(\bar{L}, Q, C) \quad (3)$$

where H_i are suitable functions and \bar{L} is the extended set of the structural parameters. Finally, combining all the mentioned equations, we can find the complete kinetostatic model described by:

$$\begin{aligned} \bar{S} = [S^T \ F^T]^T &= \bar{H}(Q, C, \bar{L}) & \bar{Q} = [Q^T \ C^T]^T &= \bar{G}(S, F, \bar{L}) \\ \bar{L} &= [L^T \ L_c^T \ L_g^T]^T \end{aligned} \quad (4)$$

where \bar{H} and \bar{G} respectively represent the direct and inverse kinetostatics of the robot, $L_c^T = [p_{ee}, p_1, p_2, \dots]^T$ is the vector of the compliance parameters, and $L_g^T = [g_{ee}, g_1, g_2, \dots]^T$ is the

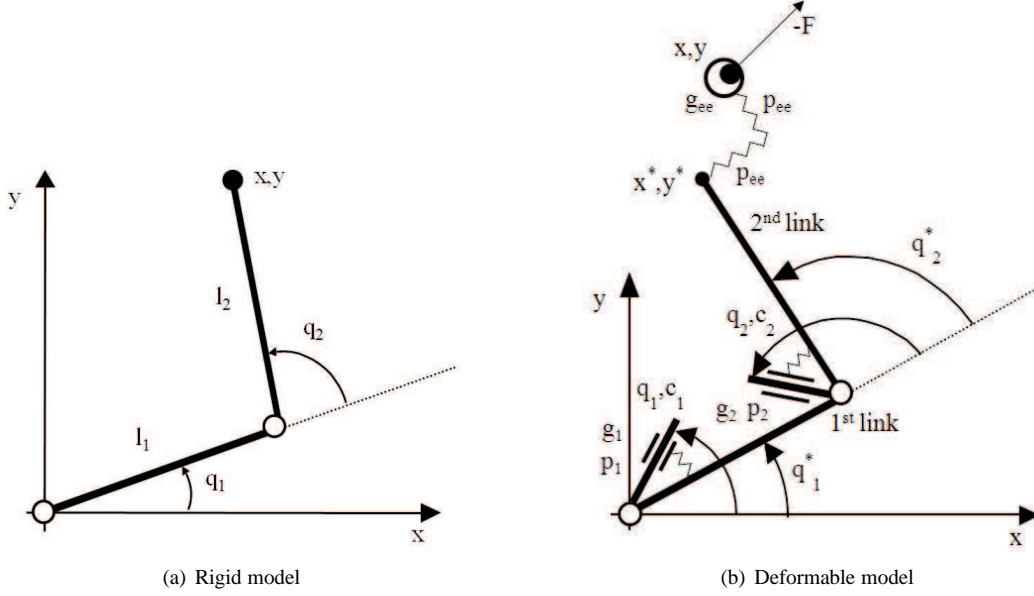


Figure 2: Comparison between the rigid and the deformable models of a planar SCARA robot.

vector of the backlashes. If some links move vertically, the influence of the gravity acceleration must be also taken into account and the vector \bar{L} must be further extended to include masses. It is important to note that in this paper we only consider static deformations, thus dynamic effects are not taken into account.

2.3 The models of the SCARA robot

In this paper, we study the case of a 2 degrees of freedom SCARA robot whose execution task is the two-dimensional *contour tracking* [7] of a planar object of unknown shape. The task is performed in the horizontal plane, so gravity is neglected. By an analysis of the task (figure 1) a planar model was considered suitable (figure 2). It is assumed that the rotation axes are both orthogonal to the x and y axes and the gripper forces are exchanged in the x - y plane.

With these considerations it is immediate to develop a rigid model (figure 2(a)) where the function H of eq. (1) and the jacobian J of eq. (2) are:

$$S = \begin{bmatrix} x \\ y \end{bmatrix} = H(L, Q) = \begin{cases} l_1 \cos(q_1 + \vartheta_1) + l_2 \cos(q_1 + q_2 + \vartheta_1 + \vartheta_2) + x_0 \\ l_1 \sin(q_1 + \vartheta_1) + l_2 \sin(q_1 + q_2 + \vartheta_1 + \vartheta_2) + y_0 \end{cases} \quad (5)$$

$$J = \begin{bmatrix} -l_1 \sin(q_1 + \vartheta_1) & -l_2 \sin(q_1 + \vartheta_1 + q_2 + \vartheta_2) \\ l_1 \cos(q_1 + \vartheta_1) & l_2 \cos(q_1 + \vartheta_1 + q_2 + \vartheta_2) \end{bmatrix}$$

with

$$L = [x_0, y_0, \vartheta_1, l_1, \vartheta_2, l_2]^T \quad Q = [q_1, q_2]^T$$

An analysis of the manipulator and of the task suggests the development of a model with deformations concentrated in the joints transmissions and in the gripper (figure 2(b)). For each joint we

define two coordinates q_i and q_i^* ($i = 1, 2$), the first describing the motion of the actuator, while the second is the motion of the link. The difference $q_i - q_i^*$ is due to the actuator torque c_i through

$$q_i - q_i^* = p_i c_i + g_i \text{sign}(c_i) \quad (6)$$

where p_i is the elastic compliance of the transmission, g_i is the half amplitude of the backlash, and sign is the signum function ($\text{sign}(t) = t/|t|$) which is equal to 1 or -1 depending on the sign of its argument and undefined for $t = 0$. Similarly the deformation of the gripper can be represented as:

$$S - S^* = \begin{bmatrix} x - x^* \\ y - y^* \end{bmatrix} = R^T \begin{bmatrix} p_{11} & p_{12} \\ p_{21} & p_{22} \end{bmatrix} R F - g_{ee} \frac{F}{\|F\|} \quad (7)$$

where R is a rotation matrix representing the orientation of the second link, p_{ij} are suitable compliance constants, g_{ee} is the gripper backlash which is supposed isotropic, and $F = [f_x, f_y]^T$. Under the hypotheses of isotropic elasticity for the gripper we get:

$$P = \begin{bmatrix} p_{11} & p_{12} \\ p_{21} & p_{22} \end{bmatrix} = \begin{bmatrix} p_{ee} & 0 \\ 0 & p_{ee} \end{bmatrix} = p_{ee} I$$

where p_{ee} represents the gripper compliance and I is the 2×2 identity matrix.

The rigid part of the manipulator is subjected to the equations described in §2.1, so

$$S^* = H(L, Q^*) \quad C = J^T F \quad (8)$$

while equations (6) and (7) may be employed to develop an explicit form of eq. (4).

On these assumptions, the complete set of the parameters necessary to describe the kinetostatic properties of the manipulator is shown in table 1. The structural parameters set consists of 12 el-

No	Parameter	Nominal value	Units	Description
1	x_0	0	[m]	Base offset x -axis
2	y_0	0	[m]	Base offset y -axis
3	ϑ_1	0	[rad]	First joint offset
4	l_1	$3.3 \cdot 10^{-1}$	[m]	First link length
5	ϑ_2	0	[rad]	Second joint offset
6	l_2	$3.3 \cdot 10^{-1}$	[m]	Second link length
7	p_{ee}	$1 \cdot 10^{-5}$	[m/N]	Gripper compliance
8	p_1	$1 \cdot 10^{-5}$	[rad/Nm]	First joint compliance
9	p_2	$1 \cdot 10^{-5}$	[rad/Nm]	Second joint compliance
10	g_{ee}	0	[m]	Gripper backlash
11	g_1	0	[rad]	First joint backlash
12	g_2	0	[rad]	Second joint backlash

Table 1: Set of the parameters for the SCARA robot.

ements divided in 3 groups: *geometric parameters*, *elastic parameters*, and *backlash*. The first six parameters form the first group and represent the robot placement (x_0 e y_0), the rotation offset on each joint (ϑ_1 e ϑ_2), and the lengths of the links (l_1 e l_2). The second group includes the joint compliances p_1 and p_2 and the gripper compliance p_{ee} , which is assumed isotropic in x and y directions. Finally, the joints backlashes g_1 and g_2 and the gripper compliance g_{ee} form the third group.

3 THE KINETOSTATIC CALIBRATION

Aim of the *calibration* is the identification of the actual values of the model parameters in order to have the possibility to compensate errors and deformations and to increase the robot accuracy [6]. In this paper we study the kinetostatic calibration [5] with a “parametric” approach “with contact” [8]. It is a new method based on the measure (provided by a force sensor installed on the gripper) of the exchanged force between the gripper and the environment and it involves the use of instrumentation available in the working cell when hybrid force-velocity control is employed.

The robot gripper is requested to touch, with a predefined force, several points of a body of known shape, called *calibration object*. At each contact point, the contact force (intensity and direction) and the joints rotations are recorded, whereas the end-effector pose can be estimated using a kinetostatic manipulator model. The calibration can be performed on the base of the difference between the measured contact force and that predicted by the model of the manipulator and of the calibration object. The deformable robot is represented by the direct and inverse kinetostatic equations described in §2.2. Note that the new calibration method is based only on the measures of F and Q and does not require the knowledge of the gripper pose S , whose accurate measure is difficult to get.

By knowing the exact position, size and shape of the calibration object and a model of the deformable manipulator it is possible to define a mathematical expression to estimate the contact force for a given value of the joints coordinates:

$$F = A(Q, \bar{L}) \quad \bar{L} = \bar{L}_n + \Delta\bar{L} \quad (9)$$

where the actual value of the parameters can be expressed as the sum of the nominal value \bar{L}_n plus an unknown deviation $\Delta\bar{L}$. In absence of contact between the end-effector and the object, the force is zero, while during the contact the force depends on the kinetostatic equations. The value of $\Delta\bar{L}$ is then estimated by minimizing a norm of the difference between the measured force and that predicted by the model (k is the number of the considered poses and e_f is an average force error) :

$$e_f = \frac{1}{k} \sum_{h=1}^k \|F_h - A(Q_h, \bar{L}_n + \Delta\bar{L})\| \quad (10)$$

4 THE NEW CALIBRATION PROCESS

4.1 Calibration objects

During the calibration process the gripper is requested to touch objects of known shape with a predefined force. Thus, one or more known objects have to be opportunely positioned in the working area and a certain number of contact points on them have to be selected. The calibration object we chose are two (or more) steel discs of different radius fixed at different distance from the robot base in order to cover a large part of the working area. The discs compliances may be included in the gripper compliance, or also neglected since we are using steel objects which are much stiffer than the robot gripper.

4.2 Kinematic and kinetostatic relations

As already mentioned in §3, the estimation of $\Delta\bar{L}$ is performed by minimizing the force error index defined in eq. (10). This evaluation is possible only if we are able to foresee the force on the gripper for given values of the joints coordinates taking into account the presence of the calibration object. More in details, it is necessary to develop a procedure that, knowing the joint position Q , the parameters \bar{L} , and the shape of the object, evaluates the actual gripper position S , the contact force F , and the torque C . This procedure is designed as described below.

The basic idea is to hypothesize, at the beginning, that the contact does not occur, meaning that forces and torques are null, so that the gripper position can be calculated by the rigid model as $S = H(L, Q)$. After this, the distance d between the gripper centre represented by S and the disc centre S_c is evaluated and compared with the disc radius r : if $d > r$ the contact does not take place and F is null, otherwise the contact position S and the contact force F depend on the kinetostatic equations. In order to evaluate them, two main conditions are considered:

- the gripper has to be on the circumference defining the disc;
- the force exerted by the robot on the disc has radial direction (null contact friction).

These conditions lead to a set of two equations in the two unknowns x and y ($S = [x, y]^T$):

$$\begin{cases} \|S - S_c\|^2 = (S - S_c)^T(S - S_c) = r^2 \Rightarrow (S - S_c)^T(S - S_c) - r^2 = 0 \\ F^T R_{90}(S - S_c) = C^T J^{-1} R_{90}(S - S_c) = 0 \end{cases} \quad (11)$$

where R_{90} is a rotation matrix rotating a vector by 90° . We remind that the contact force F depends on the manipulator pose S through equations (4) that can be particularized to the SCARA robot by equations (6) and (7). Thus, the set of equations (11) can be expanded as:

$$E = \begin{bmatrix} e_1 \\ e_2 \end{bmatrix} = \begin{cases} \lambda_1 + \lambda_2 C + C^T \lambda_3 C = e_1 \\ \lambda_4^T C + C^T \lambda_5 C = e_2 \end{cases}$$

where λ_i are suitable constants while e_1 and e_2 should be zero if the correct value of C is found. The idea is to find the joints torques C by numerical solution of eq. (11) using the iterative Newton-Raphson method. The iterative estimation is initialized assigning $C = [0, 0]^T$. Better estimations for C are found iteratively as ($k = 1, 2, \dots$)

$$C_k = C_{k-1} - J_C^+ E \quad \text{where} \quad J_C = \frac{\partial E}{\partial C}$$

and J_C^+ is the pseudoinverse of J_C .

Iterations are interrupted when $\|E\| < \varepsilon$, where ε is a suitable small positive tolerance.

4.3 Estimation of the parameters errors

In order to estimate a certain number of structural parameters at least the same number of measures is needed. Since neither the model nor the measures can be perfect, it is necessary to consider a higher number of measures and the parameters are estimated by a minimum squares criterion. The algorithm to minimize e_f is based on iterative linearization of equations (10) and (9):

$$\Delta F \simeq J_{\bar{L}} \Delta \bar{L} \quad J_{\bar{L}} = \frac{\partial A}{\partial \bar{L}} \quad (12)$$

where ΔF is the difference between the measured force and the predicted by the model and $J_{\bar{L}}$ is the jacobian matrix concerning the structural parameters.

The system is unambiguous solvable if $J_{\bar{L}}$ is invertible, whereas it gives a good estimation of $\Delta \bar{L}$ if the matrix has maximum rank and the number of rows is greater than the number of columns. In this case we assume:

$$\Delta \bar{L} = J_{\bar{L}}^+ \Delta F = (J_{\bar{L}}^T J_{\bar{L}})^{-1} J_{\bar{L}}^T \Delta F \quad (13)$$

In other words, the Newton-Raphson algorithm for the numerical solution of a non-linear set of equations is based on the iterative linearization of the equations in the neighborhood of a point that is presumed to be close to the solution. In this way, at each iteration, we get a linear system whose solution approximates the one of the non-linear set of equations. Repeating this linearization produces a series of solutions that hopefully converge to the solution of the initial set of equations:

$$\bar{L}_k = \bar{L}_{k-1} + J_{\bar{L}}^+ \Delta F \quad \bar{L}_0 = \bar{L}_n \quad (k = 1, 2, \dots) \quad (14)$$

The iterative process is interrupted when the increment of the index becomes smaller than a predefined tolerance, so that $\|\Delta F\| < \varepsilon_f$.

Notice that the Newton-Raphson algorithm is not implemented in the traditional way but it has been modified in order to fulfil the study requirements. Firstly, the inverse of the $J_{\bar{L}}$ in eq. (14) has been substituted by its pseudoinverse. Then, in order to improve the solution, two further changes have been introduced:

- the first limits the gradient by verifying that the absolute value at the $k + 1$ step is always lower than that at the k step;
- the second limits the amplitude of the maximum step.

5 RESULTS

5.1 Results of simulations

In order to check and optimize the calibration process, many simulation tests were performed. The tests were also useful to identify the minimum number of measuring points, the shape and the location of the calibration object which better guarantees a good parameters estimation. The tests were performed on a SCARA robot, simulating a calibration object formed by two or three discs of known radius and location. A “reasonable” but arbitrary set of values for \bar{L}_a was selected to represent an arbitrary manipulator. Some points located on the discs were chosen for the simulations and a value of the contact force F was selected. Then, using the function \bar{G} (eq. (4)) with $\bar{L} = \bar{L}_a$, the corresponding value of Q was evaluated. The values of Q and F for all the contact points were stored to simulate the actual measures. These values were thus reconsidered and inserted in the calibration algorithm. The resultant estimation of \bar{L} was compared with \bar{L}_a : if the procedure

Parameters	Values	Units
$[x_{c1}, y_{c1}]$	$[-0.25, 0.30]$	m
r_1	0.15	m
$[x_{c2}, y_{c2}]$	$[0.20, 0.40]$	m
r_2	0.05	m
$[x_{c3}, y_{c3}]$	$[0.05, 0.25]$	m
r_3	0.08	m
npc	12	-
f	40	N

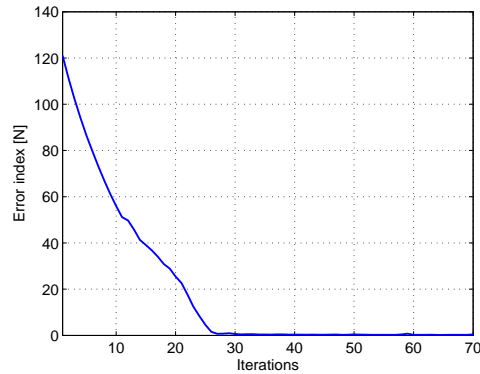


Figure 3: Example of data and results for a calibration simulation (see also table 2). The final error index (e_f) is $4.491026 \cdot 10^{-5} [N]$.

is successful it must be $\|\bar{L} - \bar{L}_a\| < \varepsilon_l$ where ε_l is a suitable small positive value. Simulations were repeated varying the number and the location of the discs, of the contact points, and of the contact force. Typical data and results are shown in figure 3 while in table 2 the estimated values are compared with those considered as “actual”. Moreover, the error index trend depending on the algorithm iterations is shown in figure 3. Tests were repeated after adding random error to the simulated measures (Q and F) to simulate measuring errors: notice that the amplitude of the added noise could be much bigger than the one detected during an actual data acquisition.

In all the cases the calibration procedure proved to converge well ($e_f \approx 10^{-5}[N]$). The error index decreases very fast to a low value: 30 iterations are generally sufficient to drastically reduce its value, but a better estimation can be achieved as the number of iterations increases. When noise is present, the contact force is predicted with an error comparable with the random error ($e_f = 1.25 \div 1.35[N]$).

Param.	“Actual” values \bar{L}_a	Estimated values \bar{L}	\bar{L} when random noise	Units
1	$2.5 \cdot 10^{-3}$	$2.500000 \cdot 10^{-3}$	$2.499527 \cdot 10^{-3}$	[m]
2	$-2.2 \cdot 10^{-3}$	$-2.199999 \cdot 10^{-3}$	$-2.202042 \cdot 10^{-3}$	[m]
3	$-1.7 \cdot 10^{-3}$	$-1.700003 \cdot 10^{-3}$	$-1.7480221 \cdot 10^{-3}$	[rad]
4	$3.302 \cdot 10^{-1}$	$3.301999 \cdot 10^{-1}$	$3.301951 \cdot 10^{-1}$	[m]
5	$7.0 \cdot 10^{-4}$	$6.999950 \cdot 10^{-4}$	$7.120833 \cdot 10^{-4}$	[rad]
6	$3.298 \cdot 10^{-1}$	$3.298000 \cdot 10^{-1}$	$3.298156 \cdot 10^{-1}$	[m]
7	$1.1 \cdot 10^{-5}$	$1.100712 \cdot 10^{-5}$	$1.541640 \cdot 10^{-5}$	[m/N]
8	$1.1 \cdot 10^{-5}$	$1.100000 \cdot 10^{-5}$	$7.951966 \cdot 10^{-6}$	[rad/Nm]
9	$1.1 \cdot 10^{-5}$	$1.100017 \cdot 10^{-5}$	$5.696328 \cdot 10^{-6}$	[rad/Nm]
10	$9.5 \cdot 10^{-5}$	$9.528501 \cdot 10^{-5}$	$2.829870 \cdot 10^{-4}$	[m]
11	$2.9 \cdot 10^{-4}$	$2.900022 \cdot 10^{-4}$	$3.869342 \cdot 10^{-4}$	[rad]
12	$2.9 \cdot 10^{-4}$	$2.899924 \cdot 10^{-4}$	$3.744674 \cdot 10^{-4}$	[rad]
Force error index e_f		$4.491026 \cdot 10^{-5}$	1.312684	[N]

Table 2: Comparison between “actual” and estimated values for the example.

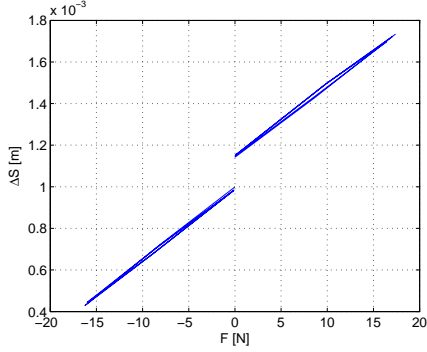
5.2 Experimental evidences for the estimation of compliance and backlash

To verify the procedure and to optimize it some experimental tests were performed on the SCARA robot installed in the Robotics Lab of the Mechanical Engineering Department of the University of Brescia. For the described SCARA robot, the compliances and the backlashes can be considered as concentrated in the gripper and in the joints and their values can be achieved through the experimental procedure described below. First of all, the evidences have been grouped in 2 main parts: the first one consisting of the estimation of the compliance and the backlash at the gripper and the second one consisting of the estimation of the same values at the joints.

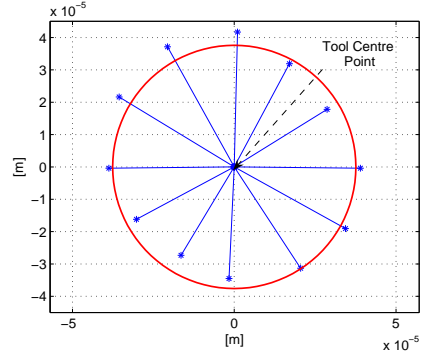
Evidences at the gripper

The experiment has been performed as follows:

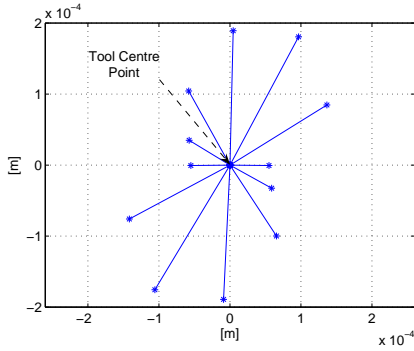
- positioning of the robot with the two links completely extended along the y axis;
- full lock of the joints rotations;
- positioning and initialization of a dial gauge touching the end-effector;
- application and subsequent removal to the end-effector of a series of progressive forces along the y direction on both sides (3 times);



(a) Typical F - ΔS graph for the gripper.



(b) Map of the gripper compliance.



(c) Map of the gripper backlash.

Gripper		
Compliance [m/N]	$3.76 \cdot 10^{-5}$	
Backlash [m]	$5.49 \cdot 10^{-5} \div 2.05 \cdot 10^{-4}$	
Joint 1		
Compliance [rad/Nm]	$3.23 \cdot 10^{-5}$	
Backlash [rad]	$2.64 \cdot 10^{-4}$	
Joint 2		
Compliance [rad/Nm]	$1.08 \cdot 10^{-4}$	
Backlash [rad]	$2.68 \cdot 10^{-4}$	

(d) Compliance and backlash values.

Figure 4: Results of the experimental analysis on the SCARA robot.

- recording of the force F [N] and of the corresponding gripper displacement ΔS [m] for each value of F ;
- repetition of the last 3 steps over 360° along directions having a constant offset of 30° .

In this way, for each direction we can draw a F - ΔS graph, one of which, as an example, is reported in figure 4(a). Then, remembering that $\Delta S = p_{ee}\Delta F$ (where p_{ee} is the gripper compliance), in each sense we can calculate the mean compliance value which represents the mean slope of the curve in the F - ΔS graph. We can also notice a gap in the ΔS values for null value of the applied force F : this means that inverting the sense of application of the force in the specific direction we caused the backlash release, whose value is the ΔS gap itself. Finally, in figure 4(b) and 4(c) are respectively drawn a map of the mean gripper compliance and the mean backlash value along all directions: notice the non-isotropy of the gripper backlash. Moreover, table in figure 4(d) reports the obtained values.

Evidences at the joints

We started from the evaluation of the compliance value p_2 and of the backlash value g_2 supposed to be concentrated in the second joint. The procedure developed into the following steps:

- positioning of the robot with the two links completely extended along the y axis;
- full lock of the rotation of the first joint;
- positioning and initialization of a dial gauge touching the end of the link 2;
- application and subsequent removal to the end-effector of a series of progressive forces along the x direction on both sides (3 times);
- recording of the force F [N] and of the corresponding displacement ΔS [m] at each value of F .

The torque applied to the joint is $F \cdot l_2$ and the joint angular displacement is $\Delta q_2 = \Delta S/l_2$. Thus, compliance and backlash are simply estimated from the collected data. An equivalent measurement procedure can be adopted to get the values of the compliance p_1 and the backlash g_1 concentrated in the first joint. Table in figure 4(d) summarizes the set of the obtained values for the two joints.

6 CONCLUSIONS

In this paper the development of a deformable model of a manipulator is presented. The system has been modelled as a chain of rigid bodies with compliance and backlash concentrated in the joints transmission and the gripper. The adoption of this model allows the realization of a kinetostatic calibration, which is necessary to achieve an accurate knowledge of the parameters describing the robot. A new calibration algorithm has been implemented, basing only on the measures of the contact force and of the joints positions and involving just the use of instrumentation usually available in the working cell when the manipulator has a force controller. The algorithm has been tested in different ways and it has always led to good results. Moreover, to check the validity of the assumption on which the model has been proposed, experimental tests for the identification of compliance and backlash in a SCARA robot have been performed (figure 4). Consequently, observing the encouraging results, our aim is to proceed with the experimental calibration, already under development, of the considered SCARA robot.

REFERENCES

- [1] Raibert, M.H. and Craig, J.J., “Hybrid Position/Force Control of Manipulators”, *ASME Journal of Dynamic Systems*, **102**, 126-133 (1981).
- [2] Omodei, A., Legnani, G. and Adamini, R., “Three Methodologies for the Calibration of Industrial Manipulators: Experimental Results on a SCARA Robot”, *J. Robotic Systems*, **17(6)**, 219-307 (2000).
- [3] Zhuang, H., Wu, J. and Huang, W., “Optimal planning of robot calibration experiments by genetic algorithms”, in *Proceedings of IEEE 1996 International Conference on Robotics and Automation*, Minneapolis, Minnesota, 981-986 (1996).
- [4] Meggiolaro, M. A., Dubowsky, S. and Mavroidis, C., “Geometric and elastic error calibration of a high accuracy patient positioning system”, *Mechanism and Mach. Theory*, **40(4)**, 415-427 (2005).
- [5] Legnani, G., Adamini, R. and Jatta, F., “Calibration of a SCARA Robot by force-controlled contour-tracking of an object of known shape”, in *Proc. of 32nd ISR*, Seoul, Korea, 510-515, April 19-21 (2001).
- [6] Mooring, B.W. and Roth, Z.S., *Fundamentals of Manipulator Calibration*, Wiley-Interscience (1991).
- [7] Ziliani, G., *Controllo dei manipolatori interagenti con l’ambiente*. PhD thesis, Università degli Studi di Brescia, Brescia, Italy (2006).
- [8] Legnani, G., *Robotica industriale*, Casa Editrice Ambrosiana, Milan, Italy (2003).